R2

Inhibition of hepatitis C virus internal ribosome entry site-mediated translation by an RNA targeting the conserved IIIf domain

*Cristina Romero-López, Raquel Díaz-González and Alfredo Berzal-Herranz**

Instituto de Parasitología y Biomedicina "López-Neyra", CSIC.

Parque Tecnológico de Ciencias de la Salud, Avda. del Conocimiento s/n, Armilla, 18100 Granada, Spain.

Running title: A small RNA blocks HCV IRES function

(*) Correspondence:

Instituto de Parasitología y Biomedicina "López-Neyra", CSIC.

Parque Tecnológico de Ciencias de la Salud, Av. del Conocimiento s/n, Armilla, 18100 Granada, Spain.

Tel.: +34 958181648; Fax: +34 958181632

E-mail: Aberzalh@ipb.csic.es

ABSTRACT

Hepatitis C virus (HCV) translation initiation depends on an internal ribosome entry site (IRES). We previously identified an RNA molecule (HH363-10) able to bind and cleave the HCV IRES region. This paper characterizes its capacity to interfere with IRES function. Inhibition assays showed that it blocks IRES activity both *in vitro* and in a human hepatoma cell line. Although nucleotides involved in binding and cleavage reside in separate regions of the inhibitor HH363-10, further analysis demonstrated the strongest effect to be an intrinsic feature of the entire molecule; the abolishment of any of the two activities resulted in a reduction in its function. Probing assays demonstrate that HH363-10 specifically interacts with the conserved IIIf domain of the pseudoknot structure in the IRES, leading to the inhibition of the formation of translationally competent 80S particles. The combination of two inhibitory activities targeting different sequences in a chimeric molecule may be a good strategy to avoid the emergence of resistant viral variants.

Keywords: Aptamer; Ribozyme; HCV targeting; RNA-based inhibitors; Gene silencing.

INTRODUCTION

Hepatitis C virus (HCV) infection affects more than 170 million people worldwide. Current treatments show poor efficacy due to the highly active dynamics of the HCV populations that promote the appearance of drug-resistant variants [1]. This problem, also faced in control of other viral infections, has prompted an intensive search for new drugs and alternative therapeutic strategies. Combination approaches are currently considered excellent candidates to reduce the chance of viral evasion.

The HCV genome is a 9500 nucleotide-long (+) ssRNA molecule. During early viral infection, uncapped viral RNAs initiate their translation using a highly conserved internal ribosome entry site (IRES) located at the 5' untranslated region (UTR; Fig. 1; [2, 3]), which includes from nt 40 to 372 of the viral genome [4, 5]. It has a complex secondary and tertiary structure that acts as a scaffold for recruiting multiple protein factors during the initiation of translation [6]. This mechanism considerably differs from that used by the cellular capped mRNAs, rendering it a potential candidate for antiviral therapies.

The use of RNA molecules as gene inactivation agents is a therapeutic option that has been investigated in depth [7]. Antisense RNAs and siRNAs have been proved to effectively inhibit replication of several viruses, including HCV [8]. These molecules work by sequence complementarity and in many cases viruses promptly escape to the treatment [9-13]. Viral targeting with other RNA molecules like ribozymes and aptamers has also been accomplished with different success [8]. In contrast to antisense and siRNAs, aptamers do not operate only by sequence complementarity, but also by the recognition of secondary and tertiary structures. The formation of productive complexes is a major requisite for the correct functioning of aptamers and ribozymes too. These features

contribute to diminish the chance of appearance of resistant viral mutants. An additional issue to minimize the risk of the emergence of escape variants is the use of several inhibitors with different specificities [14-16]. We previously designed a novel combined approach [17]. An *in vitro* selection method was employed to isolate a collection of RNA molecules composed of a hammerhead ribozyme (named HH363) targeting positions 357-369 of the HCV genome, plus an aptamer for the 5'UTR that carries a domain complementary to unique sequences in the IRES domain [17]. In this paper, the selected variants have been assayed for their ability to interfere with IRES function. This has allowed the identification of a very potent inhibitor designated as HH363-10, which behaves as an aptamer with complementary sequences to domain IIIf of the 5'UTR (Ap10; Fig. 1; [17]). This region participates in the formation of a pseudoknot structure essential for IRES function [18]. It has been proposed that the IIIf domain interacts with the 40S ribosomal subunit [19, 20] and favors the formation of active translational 80S complexes [21]. This paper is the first to report an RNA molecule that combine two functional modules that interact with different regions of the HCV IRES, interfering with its function both *in vitro* and in a human liver cell line.

MATERIALS AND METHODS

DNA templates and RNA synthesis

All RNAs were synthesized by *in vitro* transcription and purified as previously described [22]. DNA templates for the HCV-derived RNAs 5'HCV-691 and 5'HCV-691gg were obtained as previously described [17]. The template for RNA 667 was derived from the pcDNA3 vector (Invitrogen) linearized with *Dra*III. The coding sequence for IRES-FLuc

was obtained by PCR amplification of the plasmid pCMVCatIREcLuc [17]. The pRLSV40 vector (Promega) was linearized with *Bam*H1 for the synthesis of RLuc mRNA.

The DNA templates for the HH363-10 and HH363 inhibitory RNAs were obtained as described in [17]). The dsDNAs used for the synthesis of Ap10, HH363m-10, HH363-10m and HH363m-10m were generated by annealing and extension as previously described [23], of oligonucleotide T7GG (5'-taatacgactcactatagg-3') with T7Ap10 (5'-GTAGGATTACGAATCACTCAGAAcctatagtgagtcgtatta-3'), 5'T7HH363m (5'-TAATACGACTCACTATAGGGTTCTTTCTGATAAGTCCGTgaggacgaaaggttt-3') with asHH363-10 (5'-GCTGAAAGCTTGGATCCGCTCAGTAGGATTACGAATCACTCAGAAaaacctttcgtcctc-3'), 5'HH363is (5'-TATGAATTCTAATACGACTCACTATAGGGTTCTTTCTGATGAGTCCGTgaggacgaaaggttt-3') with asHH363-10m (5'-GCTGAAAGCTTGGATCCGCTCAGTAGGATGTGCAATCACTCAGAAaaacctttcgtcctc-3'), and 5'T7HH363m (5'-TAATACGACTCACTATAGGGTTCTTTCTGATAAGTCCGTgaggacgaaaggttt-3') with asHH363-10m (5'-GCTGAAAGCTTGGATCCGCTCAGTAGGATGTGCAATCACTCAGAAaaacctttcgcctc-3'; the T7 promoter sequence is underlined; lower case letters indicate the complementary sequences). The plasmid pBSSK was digested with the restriction enzyme *Bam*H1 for the synthesis of RNA_{80}.

The RNA molecules employed in the inhibition assays were obtained using the RiboMAX^{TM}-T7 large scale RNA production system (Promega); the manufacturer's instructions were strictly followed. The transcription mix of IRES-FLuc was supplemented

with 200 μCi of α-^{32}P-UTP for ribosome assembly assays. During the synthesis of the RNA RLuc, a cap structure was incorporated into its 5' end by adding 5 mM of Ribo m^7G Cap Analog (Promega). The resulting RNAs were purified by phenol extraction and unincorporated nucleotides were removed by two consecutive steps of size exclusion chromatography (Sephadex G-25, GE Healthcare). The RNA amount was determined by A_{260} measurements, and the extent of protein and carbohydrate/phenolic contaminations was assessed by A_{260}/A_{280} and A_{260}/A_{230} ratios, respectively. The integrity of the RNA was determined by agarose-formaldehyde gel electrophoresis.

***In vitro* translation assays**

IRES-FLuc and RLuc mRNAs were translated using the Flexi® rabbit reticulocyte lysate system (Promega). Reactions proceeded in 6 μl volumes containing 4 μl of cell extract, 0.1 μl of the provided aminoacid mixture lacking methionine (1mM), and 0.1 μl (1.5 μCi) of a mixture of L-(^{35}S)-methionine and L-(^{35}S)-cysteine (Redivue Pro-mix L-(^{35}S) *in vitro* cell labeling kit, GE Healthcare). KCl was supplemented at 100 mM. The RNA templates for the synthesis of either FLuc (IRES-FLuc) or RLuc (RNA RLuc) proteins were added at a final concentration of 30 ng/μl (~ 40 nM) and 20 ng/μl (~ 60 nM) respectively. Inhibitory RNA concentrations ranging from 10 nM to 5 μM were assayed. All the RNA molecules were subjected to a denaturing step at 65ºC for 10 min and subsequently incubated at 4ºC for 15 min prior to their incorporation into the translation mix. Translation proceeded at 30ºC for 60 min. Reactions were stopped on ice and the protein products resolved on 12.5% (w/v) denaturing polyacrylamide gels. Dried gels were scanned in a Phosphorimager (Storm 820, GE Healthcare) and quantified with Image Quant 5.2© software (GE Healthcare). The IC_{50} values were calculated with SigmaPlot 8.02© software using the

equation $y = y_{max}/(1 + 10^{(LogIC_{50}-X)})$, where y_{max} is the maximum percentage of FLuc relative synthesis, IC_{50} the inhibitor concentration that produces 50% of the maximum observed effect, and X the inhibitor concentration.

IRES cleavage assays

Cleavage experiments proceeded in the presence of RRL under *in vitro* translation reaction conditions. All were performed in the presence of 40 nM ^{32}P-internally radiolabeled RNA substrate 5'HCV-691. Substrates and inhibitor RNAs were denatured and renatured as described above. After 60 min at 30ºC, reactions were stopped on ice and the RNA molecules were phenol-extracted. Cleavage products were resolved on 4% denaturing polyacrylamide gels, which were subsequently dried and analyzed as above.

RNA-RNA interaction probing assays

RNA probing assays of the complex HH363-10/IRES were performed with ^{32}P 5' end-labeled inhibitor RNA. Complexes were constructed as described in [17] by incubating 50 fmol of the ^{32}P 5'-end-labeled HH363-10 (~ 500 CPM) with 20 pmol of non-labeled HCV RNA. Control reactions were performed in the presence of a non-related RNA (RNA 667). Digestion reactions were initiated by the addition of RNase T1 (0.1 units), RNase A (0.2 ng) or Pb^{2+} acetate (15 mM), and incubated at 4ºC for 2 min, 30 min and 20 min respectively. An equal volume of denaturing loading buffer supplemented with EDTA 100 mM was added, and the products resolved on high resolution denaturing polyacrylamide gels (8-20%). These were dried and scanned as above.

For RNase H-mediated degradation, 50 fmol of the ^{32}P 5'-end-labeled 5'HCV-356 (~ 500 CPM) were incubated with 20 pmol of non-labeled inhibitor in the presence of 20 pmol of

the oligonucleotide asIRES305 (5'-ACTCGCAA-3') or asIRES196 (5'-TATCCAAGA-3'). Complexes were basically formed as described [17]. A final RNase H (USB) concentration of 5 U/µl was used to initiate the degradation. Digestion reactions were incubated for 10 min at 37ºC and stopped on ice. Specific products were resolved on 6% high resolution denaturing polyacrylamide gels, dried, and scanned as described above.

Ribosome-IRES complex assembly assays

The identification of 48S and 80S particles was essentially performed as described by Ray *et al*. [24]. Briefly, a concentration of 40 nM of ^{32}P-internally labeled RNA IRES-FLuc (~200,000 dpm) was incubated with 5 µM of the inhibitor RNAs and 5 µl of a translation reaction mix containing 4 µl of RRL. To prevent the formation of the 80S particle, the translation mix was supplemented with 2 mM of 5'-guanylyl imidophosphate (GMP-PNP, Sigma Aldrich). The reactions were incubated at 30ºC for 60 min and stopped on ice. The mixtures were then diluted to 150 µl with gradient buffer (20 mM Tris-HCl pH 7.5, 100 mM KCl, 3 mM $MgCl_2$, 1 mM DTT) and loaded onto a continuous 10-30% linear sucrose gradient. Ribosomal complexes were resolved by ultracentrifugation at 30,000 rpm for 4 h in a SW40 Ti rotor. Fractions of 500 µl were collected from the top of the gradient and their radioactivity was measured using a QuickCount QC-4000/XER Benchtop Radioisotope Counter (Bioscan, Inc.).

Transfection of RNA molecules into Huh-7 cells

Human hepatoma cells (Huh-7) were grown in Dulbecco's modified Eagle medium (DMEM) supplemented with 10% heat-inactivated fetal bovine serum (FBS; Invitrogen) and 2 mM of L-glutamine (Sigma), at 37º C in a 5% CO_2 atmosphere. Thirty hours before

transfection, 120,000 cells were seeded onto a 24-well plate. A mix containing 1 μg of the mRNA IRES-FLuc, 0.5 μg of RLuc, 50 μl of Opti-MEM® (Invitrogen) and 1.5 μl of transfection reagent (TransFectin^{TM}, Bio-Rad) was complemented with 50 μl of Opti-MEM®, with or without inhibitor RNA. The amounts of inhibitor employed in these assays were established at 0.7, 1.4, 2.7, 4 and 5.4 μg. The total amount of RNA was the same for all transfections (7 μg); this was achieved by complementing with a non-related 80 nt long RNA molecule (RNA_{80}). RNA molecules were denatured, and then renatured, before transfection as above. The lipid-RNA complex was added to the Huh-7 cells and incubated for 18 h at 37º C [25]. *Firefly* and *Renilla* luciferase activities were determined using the Dual-Luciferase^{TM} reporter assay system (Promega).

RESULTS

In vitro inhibition of IRES-dependent translation by a collection of chimeric RNAs

We previously described the isolation by *in vitro* selection of a collection of 30 RNA molecules that specifically target the HCV IRES [17]. All the selected variants were classified in seven families defined by common sequence motifs. One representative of each group was analyzed for its ability of interfering with IRES function in coupled transcription-translation systems. A significant inhibitory activity was detected for the seven tested molecules [17].

To further survey the potential IRES-inhibition function of each selected variant and to exclude any non-specific effect over transcription, *in vitro* translation assays of monocistronic IRES-FLuc and cap-RLuc mRNAs have been performed using rabbit reticulocyte lysates (RRL) in the presence of the different inhibitor RNAs. IRES activity

was measured as the synthesis of FLuc protein and compared to the levels of RLuc, which is translated in a cap-dependent manner. All the molecules inhibited IRES function at a concentration of 5 μM, some of them by as much as 90% (Fig. 2). The difference in the experimental approach (translation instead of transcription-translation) might explain the apparent discrepancies in the observed inhibition data presented here and those previously published [17]. No significant effect was seen on cap-dependent translation (<5%, data not shown) for any of the assayed molecules at the concentration tested, indicating a selective inhibition of IRES function. Since all the RNA molecules shared the HH363 domain, presumably both the targeting site of the aptamer and the structure of the whole inhibitory molecule are associated with the potency of each inhibitor.

HH363-10 potently interferes with IRES-dependent translation *in vitro*

We focused on HH363-10, which strongly blocked IRES-dependent translation by up to 90% (Fig. 2). The aptamer sequence contains a motif complementary to the highly conserved domain IIIf of the HCV 5'UTR (Fig. 1; [17]), suggesting it to be a possible interaction site. This observation led us to study in detail its activity in *in vitro* translation assays. Several concentrations of HH363-10 were tested, ranging from a molar ratio IRES-FLuc:HH363-10 of 4:1 to 1:125. Strong, dose-dependent inhibition of IRES-dependent translation was observed, with an IC_{50} value of 150 nM (Fig. 3 and Table 1). Further, at the lowest concentration of the inhibitor tested, a significant reduction in the FLuc levels was achieved (around 20%). This effect was specific for IRES-dependent translation, since the synthesis of RLuc protein was not affected even at the highest concentrations assayed (<5%, data not shown). To corroborate the specificity of HH363-10 for the HCV IRES, a control experiment was performed in which the synthesis of FLuc protein was mediated by

the EMCV IRES and normalized with respect to RLuc levels. No significant changes in IRES activity were detected in the presence of HH363-10 (Fig. 3), validating its potential as a specific HCV IRES inhibitor.

The contribution of the two activities (cleavage by HH363 and binding by Ap10) to the inhibitory capacity of the chimeric molecule was further analyzed. Although they both clearly reduced FLuc levels on their own in a dose-dependent manner, their action was significantly less than that exerted by the entire HH363-10 molecule at every assayed concentration (Fig. 3 and Table 1). A fall in inhibitory activity was also observed (as well as a 12-fold increase in the IC_{50} value) when both HH363 and Ap10 were simultaneously added to the translation reaction. This indicates that the combination of the two inhibitory domains in a single molecule is required to reach the strongest inhibition.

Cleavage of RNA IRES by HH363-10

The capacity of HH363-10 for processing IRES RNA was previously *in vitro* analyzed in the absence of any protein factor. A molecule containing the first 691 nucleotides of the HCV-1b genome (5'HCV-691; [17]), that comprised the whole IRES to allow ribosome assembly and translation [4] was specifically cleaved at the expected site (Romero-López *et al*., unpublished data). We wanted to explore the HH363-10 capacity of processing the HCV IRES in the presence of translation factors. For this purpose, a concentration of 40 nM of the internally radiolabeled 5'HCV-691 RNA was incubated with different amounts of HH363-10 in rabbit reticulocytes lysates (RRL), as explained in Materials and methods. The proportion of the specific cleavage products increased with increasing amounts of the catalytic RNA, showing a concentration-dependent effect (Fig. 4). Cleavage activity was compared with the one of HH363. It showed a slight reduction in the amount of the reaction

products in comparison to the chimeric inhibitor (Fig. 4). The improvement in the processing efficiency of HH363-10 in RRL with respect to HH363 may partially reflect the enhancement of the inhibition detected for the chimeric inhibitor.

Identification of the interacting sites between HH363-10 and the IRES region

We previously identified a sequence within the aptamer, A_{46}UUCGUAA_{53}, complementary to the IRES IIIf domain (Fig. 1; [17]), suggesting its involvement in the interaction with the IRES. Secondary structure analysis and experimental mapping of the residues involved in the interaction was undertaken to validate this hypothesis.

We firstly proceeded to determine the interacting sequence in the IRES region. For this purpose, a 5'-end radiolabeled RNA containing the full 5'UTR was used as a substrate (5'HCV-356; [17]). RNase H probing assays were performed using a 9-mer DNA oligonucleotide, asIRES305, complementary to the loop of domain IIIf (see Materials and methods). A specific RNase H cleavage product with the expected length was identified (305 nt; Fig. 5A). Increasing amounts of HH363-10 promoted a significant and dose-dependent reduction in the amount of the degradation product (Fig. 5A, C). This indicates that domain IIIf is involved in the binding between the chimeric inhibitor and the IRES. No effect on the RNase H cleavage pattern was observed when a DNA oligonucleotide complementary to positions 196-204 of the HCV genome was used in the presence of HH363-10 (asIRES196; Fig. 5B, C), demonstrating the specificity of the interaction.

RNase and lead probing assays were subsequently performed to analyze the secondary structure of HH363-10 and to identify the residues involved in the association to domain IIIf. The inhibitor RNA was 5' end-labeled with ^{32}P and incubated with a molar excess of a non-related RNA (RNA 667). Partial digestion with nucleases (RNase T1 and RNase A)

and lead was subsequently performed. Cleavage mainly occurred at specific single stranded positions (G nucleotides for RNase T1 probing, C or U residues for RNase A reactions and any nucleotide for lead treatments). The degradation pattern of HH363-10 was used for secondary structure predictions using Mfold software [26]. This showed the exposure of nucleotides A_{46}UUCGUAA_{53} in an apical loop (Fig. 1B, Fig. 6). Further *in silico* structural analyses with the PknotsRG program predicted the formation of an intramolecular pseudoknot involving the nucleotides A_{46} to G_{50} and C_{63} to U_{67} (Fig. 1B, Fig. 6).

The results were compared with those in the presence of the IRES to map the residues involved in the interaction. RNA 5'HCV-691gg was used as a substrate. This extends to nucleotide 691 of the HCV-1b genome sequence, but contains two substitutions (U_{362}→G and C_{363}→G) that completely abolish cleavage by the catalytic domain HH363 [27, 28]. The results showed nucleotides G_{45} to C_{49} to be now clearly resistant to cleavage (Fig. 6), suggesting their involvement in the interaction of HH363-10 with the IRES. Further, residues C_{63} to U_{67} showed greater sensitivity to the hydrolytic reagents in the presence of the substrate 5'HCV-691gg. This was in good agreement with the formation of an intramolecular pseudoknot structure in the inhibitor.

These results confirm the initial hypothesis that the IIIf domain is the interaction site for HH363-10. To our knowledge, this is the first report describing an RNA aptamer targeting the HCV IRES pseudoknot motif.

HH363-10 prevents the assembly of the 80S ribosomal complex

Domain IIIf of HCV IRES has been suggested a crucial motif for the recruitment of the 40S ribosomal subunit in the formation of the 48S particle. It is also reported to be involved in the subsequent structural RNA IRES rearrangements that finally lead to the formation of

an active 80S translational complex [19, 29, 30]. The effect of HH363-10 on HCV IRES-mediated ribosome assembly was therefore examined. For this purpose, *in vitro* translation reactions containing ^{32}P-labeled mRNA IRES-FLuc were performed either in the presence or absence of a 125-fold molar excess of HH363-10. The 48S and 80S particles were analyzed by sucrose density gradient ultracentrifugation (see Materials and methods). After fractioning, they were detected as two different and well-defined peaks when no inhibitor was added (Fig. 7). Experimental conditions were established to achieve the reproducibility in the efficiency of the complexes 48S and 80S formation in the absence of inhibitor. The addition of HH363-10 reduced the formation of the 80S complex, whereas the 48S particle was clearly produced (Fig. 7). These data were confirmed in a subsequent independent assay (data not shown). A similar result was obtained when reactions were incubated with GMP-PNP, a non-hydrolysable GTP analog that blocks the progression of a translation initiation complex at the 48S particle stage (Fig. 7). Similarly, an evident reduction in 80S complex accumulation was detected in the presence of Ap10 (Fig. 7), while no significant changes were observed when HH363 was present (Fig. 7). These observations suggest that the prevention of 80S particle formation is related to the inhibition exerted by HH363-10 and Ap10; this inhibition is explained by their binding to the IIIf domain.

Inhibition of IRES function by HH363-10 in a human liver cell line

The effect of HH363-10 on IRES function in cell culture was also examined. A mixture of the IRES-FLuc and cap-RLuc transcripts was co-transfected with HH363-10 into a hepatocellular carcinoma cell line (Huh-7) that supports efficient HCV replication. A dose-dependent study was performed to determine the activity of the inhibitor. HH363-10 appeared as an effective and specific inhibitor of IRES-dependent translation, reducing

FLuc activity by up to 50% at 300 nM (Fig. 8) without affecting to that shown by RLuc (<5%; data not shown).

Since the strongest inhibitory effect resides in the complete molecule, a collection of mutants was constructed to further study the contribution of the cleavage and binding activities to the inhibitory function of HH363-10 (Fig. 1B). This included a catalytically non-active derivative (HH363m-10), a null variant for the interaction site in the aptamer (HH363-10m), and a completely inactive molecule containing both modifications (HH363m-10m; Fig. 1B). These mutations involve a small number of changes in the nucleotidic sequence, but they entail a complete loss of function. Modifications in the catalytic core led to a full loss of cleavage activity and mutations in the aptamer domain completely abolished association with the IRES (data not shown). Inhibition assays showed that functionality in cells was also severely affected by these mutations. Single mutants mildly inhibited IRES-dependent translation, whereas no inhibitory effect was observed for the HH363m-10m construct. This result suggests that the strongest inhibitory activity is an intrinsic feature of the entire HH363-10 molecule combining both activities.

DISCUSSION

The search of novel therapeutic strategies to fight against HCV infection is a major goal. The high variation rate of the viral genome leads to the appearance of populations consisting of a spectrum of genomic sequences, in which resistant variants to treatment emerge and contribute to the progression of the disease [1]. In recent years, this has been outlined as the main difficulty to achieve effective therapies and has imposed the necessity of searching new targets. Classical medical approaches targeting essential HCV proteins

were considered excellent strategies for a long time. However, mutations conferring resistance to the treatment were finally reported [31]. Efforts were subsequently focused on interfering with highly conserved genomic regions. The great advances in the antisense and siRNA technology prompted the idea of an efficacious therapy in the near future, but in many cases the emergence of resistant viral genomes was certainly observed for this and other viral infections [9-13]. One of the most promising approaches is the specific recognition of highly structured regions in the genomic RNA that retain an important sequence and structure conservation rate and fulfill essential roles in viral translation and replication. They interact with viral and host proteins to carry out these crucial functions for the viral maintenance and propagation. This means that the assessment of both primary and secondary structure in those RNA domains is crucial for the conservation of the function [18]. It has been shown that mutations that preserve the secondary structure also result in a drastic reduction of the *in vitro* translation efficiency [18]. This is in good agreement with the high sequence conservation observed in this domain among different HCV isolates [32]. In this context, targeting the HCV IRES region is an excellent therapeutic option. The use of ribozymes and aptamers as anti-HCV agents has been extensively reported [8]. Aptamers are considered an excellent option to target highly folded RNA domains [33-35]. In contrast to antisense, which interaction with complex structured domains is severely restricted, aptamers only require a short stretch of complementary nucleotides in an appropriate structural context to exhibit the highest affinity and efficiency. Further, the development of combination therapies using antiviral compounds with different specificities would additionally contribute to prevent the emergence of resistant viral pools [1, 14, 15]. The functional characterization of HH363-10, which simultaneously targets two highly conserved regions that are required for the

preservation of the IRES activity [18, 36, 37], clearly shows the advantage of combining two inhibitory activities in a single molecule to achieve the strongest effect and allows the proposal of our strategy as an excellent start point for the development of new therapeutic tools.

The chimeric RNA HH363-10 strongly inhibited HCV IRES-dependent translation *in vitro*, with an IC_{50} of 150 nM. This value is considerably lower than those reported for a decoy RNA of the stem-loop IIIe-f and for two aptamers of the IRES targeting domains II and IIId [24, 33, 35] but slightly higher than other obtained for an antisense RNA of the IIId domain [25]. Since HH363-10 combines two inhibitory activities targeting different domains of the HCV genome, it might result in a more effective anti-HCV agent, though this would require further analysis.

HH363-10 also showed inhibitory activity of the HCV IRES function in a hepatoma cell line, though to a less extent that *in vitro*. This discrepancy has been previously reported [24]. Ray and Das described differences in the inhibition of HCV IRES exerted by small RNAs between *in vitro* and in cell culture experiments. Further, they reported different inhibition levels in two cell lines, Hela and Huh-7, under similar experimental conditions. It has also been shown that HCV-IRES activity is dependent on the concentration of different translation trans-acting factors. Salt concentrations and the cell cycle phase may influence the HCV-IRES efficiency [38-40]. Differences in inhibition levels can also be the result of the different concentrations of RNA at the right cellular compartment compared to the *in vitro* experiments.

It is noteworthy that the activity of the entire molecule is significantly more potent than that measured for the components as independent molecules, HH363 and Ap10. This is consistent with the fact that Ap10 was isolated by the *in vitro* selection process attached to

HH363. This, together with the fact that mutations that block either the catalytic activity of the hammerhead ribozyme or the association via the aptamer domain negatively affect the inhibitory capacity of HH363-10, highlight the need for the selected full-length molecule conserving both inhibitory activities if maximum inhibition is to be attained. Although only a low proportion of specific cleavage products are generated by the HH363-10 in RRL, the abolishment of the catalytic activity negatively influences the inhibitory properties of HH363-10, meaning that it contributes to the global inhibitory effect, though to a low extent. Besides the cleavage activity, we cannot discard a possible antisense effect of the catalytic domain. It is also likely that a structural stabilization of the aptamer domain is mediated by the HH363 motif. An improvement in the access to the domain IIIf is feasible too. We suggest that the binding of HH363-10 to its target is the key step in its mechanism of action, and that the recognition of the primary, secondary and tertiary structure in the substrate is the essential point to achieve the effectiveness of the inhibitor. None of these possibilities can be ruled out; neither are they mutually exclusive. Other explanations may also be possible. We argue that observed inhibition is an intrinsic property of HH363-10 and we cannot define the exact contribution of each activity. It should be also noted that the combination of both inhibitory activities may contribute to reduce the chance of appearance of resistant viral pools.

The results show that domain IIIf of the HCV IRES is involved in the interaction with HH363-10 (Fig. 5). To our knowledge, this is the first report describing an RNA aptamer that specifically interacts with the pseudoknot structure of the HCV IRES. We have not any information about the nature of this interaction. Nucleotides involved in the association between the inhibitor and the substrate map in apical loops (Fig. 5, Fig. 6). It would be therefore plausible that tertiary restricted kissing interactions are established. Since domain

IIIf participates in the formation of a pseudoknot structure, it seems likely that an additional contribution is required to destabilize this motif and promote the kissing between HH363-10 and the IRES. We hypothesize that residues $G_{41}A_{42}G_{43}$, complementary to positions 325 to 327 at the 3'end of the pseudoknot structure in the IRES, are working in that way. This is supported by the fact that they show a decrease in their sensitivity to RNases mediated cleavage in the presence of the substrate RNA (Fig. 6). From a structural and functional point of view, these results are of clear interest. Domain IIIf shows strong sequence and structure conservation among different isolates and has an important role in IRES function [18-20]. It has been described that distortions in its architecture dramatically affect viral polyprotein translation [18]. All these features make it an excellent target for HCV inactivation assays. The present data show that, as a result of the association of HH363-10 to IRES through the IIIf domain, the formation of the 80S particle *in vitro* is almost completely abolished (Fig. 7), which may explain the inhibitory activity of HH363-10.

In summary, the combination of antiviral agents with different specificity and activity in a sole molecule is a novel strategy that could provide a good way of restraining the emergence of resistant variants and may be extended to other viral infections, such as HIV. The anti-IRES properties shown by HH363-10 both *in vitro* and in cell culture call for its mechanism of action and activity in viral culture systems to be thoroughly investigated. Work in this area is currently underway at our laboratory. Finally, this chimeric molecule has potential as a biochemical tool for studying RNA-RNA interactions and investigating the role of the pseudoknot structure in the HCV cycle.

ACKNOWLEDGEMENTS

We thank Drs. Alicia Barroso-delJesus, Carlos Briones, Encarnación Martínez-Salas and Jordi Gómez for helpful discussions and suggestions. We also thank Vicente Augustin for excellent technical assistance. This work was supported by grant BFU2006-02568 from the Spanish *Ministerio de Educación y Ciencia* and CTS-233 from the *Junta de Andalucía* to A. B-H. C. R-L was funded by grant BMC2003-669. R. D-G was the recipient of a fellowship from the Spanish *Ministerio de Educación y Ciencia*.

REFERENCES

1 Domingo E., and Gómez J. (2007) Quasispecies and its impact on viral hepatitis. Virus Res. 127, 131-150

2 Tsukiyama-Kohara K., Iizuka N., Kohara M., and Nomoto A. (1992) Internal ribosome entry site within hepatitis C virus RNA. J Virol. 66, 1476-1483

3 Wang C., Sarnow P., and Siddiqui A. (1993) Translation of human hepatitis C virus RNA in cultured cells is mediated by an internal ribosome-binding mechanism. J Virol. 67, 3338-3344

4 Reynolds J. E., Kaminski A., Carroll A. R., Clarke B. E., Rowlands D. J., and Jackson R. J. (1996) Internal initiation of translation of hepatitis C virus RNA: the ribosome entry site is at the authentic initiation codon. Rna. 2, 867-878

5 Wang T. H., Rijnbrand R. C., and Lemon S. M. (2000) Core protein-coding sequence, but not core protein, modulates the efficiency of cap-independent translation directed by the internal ribosome entry site of hepatitis C virus. J Virol. 74, 11347-11358

6 Kieft J. S., Zhou K., Jubin R., Murray M. G., Lau J. Y., and Doudna J. A. (1999) The hepatitis C virus internal ribosome entry site adopts an ion-dependent tertiary fold. J Mol Biol. 292, 513-529

7 Puerta-Fernández E., Romero-López C., Barroso-delJesus A., and Berzal-Herranz A. (2003) Ribozymes: recent advances in the development of RNA tools. FEMS Microbiol Rev. 27, 75-97

8 Romero-López C., Sánchez-Luque F. J., and Berzal-Herranz A. (2006) Targets and tools: recent advances in the development of anti-HCV nucleic acids. Infect Disord Drug Targets. 6, 121-145

9 Boden D., Pusch O., Lee F., Tucker L., and Ramratnam B. (2003) Human immunodeficiency virus type 1 escape from RNA interference. J Virol. 77, 11531-11535

10 Das A. T., Brummelkamp T. R., Westerhout E. M., Vink M., Madiredjo M., Bernards R., and Berkhout B. (2004) Human immunodeficiency virus type 1 escapes from RNA interference-mediated inhibition. J Virol. 78, 2601-2605

11 Westerhout E. M., Ooms M., Vink M., Das A. T., and Berkhout B. (2005) HIV-1 can escape from RNA interference by evolving an alternative structure in its RNA genome. Nucleic Acids Res. 33, 796-804

12 Konishi M., Wu C. H., Kaito M., Hayashi K., Watanabe S., Adachi Y., and Wu G. Y. (2006) siRNA-resistance in treated HCV replicon cells is correlated with the development of specific HCV mutations. J Viral Hepat. 13, 756-761

13 Sabariegos R., Giménez-Barcons M., Tápia N., Clotet B., and Martínez M. A. (2006) Sequence homology required by human immunodeficiency virus type 1 to escape from short interfering RNAs. J Virol. 80, 571-577

14 Macejak D. G., Jensen K. L., Pavco P. A., Phipps K. M., Heinz B. A., Colacino J. M., and Blatt L. M. (2001) Enhanced antiviral effect in cell culture of type 1 interferon and ribozymes targeting HCV RNA. J Viral Hepat. 8, 400-405

15 Jarczak D., Korf M., Beger C., Manns M. P., and Kruger M. (2005) Hairpin ribozymes in combination with siRNAs against highly conserved hepatitis C virus sequence inhibit RNA replication and protein translation from hepatitis C virus subgenomic replicons. Febs J. 272, 5910-5922

16 Korf M., Jarczak D., Beger C., Manns M. P., and Kruger M. (2005) Inhibition of hepatitis C virus translation and subgenomic replication by siRNAs directed against highly conserved HCV sequence and cellular HCV cofactors. J Hepatol. 43, 225-234

17 Romero-López C., Barroso-delJesus A., Puerta-Fernández E., and Berzal-Herranz A. (2005) Interfering with hepatitis C virus IRES activity using RNA molecules identified by a novel in vitro selection method. Biol Chem. 386, 183-190

18 Wang C., Le S. Y., Ali N., and Siddiqui A. (1995) An RNA pseudoknot is an essential structural element of the internal ribosome entry site located within the hepatitis C virus 5' noncoding region. Rna. 1, 526-537

19 Lytle J. R., Wu L., and Robertson H. D. (2002) Domains on the hepatitis C virus internal ribosome entry site for 40s subunit binding. Rna. 8, 1045-1055

20 Lyons A. J., Lytle J. R., Gomez J., and Robertson H. D. (2001) Hepatitis C virus internal ribosome entry site RNA contains a tertiary structural element in a functional domain of stem-loop II. Nucleic Acids Res. 29, 2535-2541.

21 Fraser C. S., and Doudna J. A. (2007) Structural and mechanistic insights into hepatitis C viral translation initiation. Nat Rev Microbiol. 5, 29-38

22 Barroso-delJesus A., Tabler M., and Berzal-Herranz A. (1999) Comparative kinetic analysis of structural variants of the hairpin ribozyme reveals further potential to optimize its catalytic performance. Antisense Nucleic Acid Drug Dev. 9, 433-440.

23 Barroso-delJesus A., Puerta-Fernández E., Tápia N., Romero-López C., Sánchez-Luque F. J., Martínez M.-A., and Berzal-Herranz A. (2005) Inhibition of HIV-1 replication by an improved hairpin ribozyme that includes an RNA decoy. RNA biology. 2, 75-79

24 Ray P. S., and Das S. (2004) Inhibition of hepatitis C virus IRES-mediated translation by small RNAs analogous to stem-loop structures of the 5'-untranslated region. Nucleic Acids Res. 32, 1678-1687

25 Tallet-López B., Aldaz-Carroll L., Chabas S., Dausse E., Staedel C., and Toulmé J. J. (2003) Antisense oligonucleotides targeted to the domain IIId of the hepatitis C virus IRES compete with 40S ribosomal subunit binding and prevent in vitro translation. Nucleic Acids Res. 31, 734-742

26 Zuker M. (2003) Mfold web server for nucleic acid folding and hybridization prediction. Nucleic Acids Res. 31, 3406-3415

27 Ruffner D. E., Stormo G. D., and Uhlenbeck O. C. (1990) Sequence requirements of the hammerhead RNA self-cleavage reaction. Biochemistry. 29, 10695-10702.

28 Kore A. R., Vaish N. K., Kutzke U., and Eckstein F. (1998) Sequence specificity of the hammerhead ribozyme revisited; the NHH rule. Nucleic Acids Res. 26, 4116-4120

29 Kieft J. S., Zhou K., Jubin R., and Doudna J. A. (2001) Mechanism of ribosome recruitment by hepatitis C IRES RNA. Rna. 7, 194-206

30 Ji H., Fraser C. S., Yu Y., Leary J., and Doudna J. A. (2004) Coordinated assembly of human translation initiation complexes by the hepatitis C virus internal ribosome entry site RNA. Proc Natl Acad Sci U S A. 101, 16990-16995

31 Wohnsland A., Hofmann W. P., and Sarrazin C. (2007) Viral determinants of resistance to treatment in patients with hepatitis C. Clin Microbiol Rev. 20, 23-38

32 Bukh J., Purcell R. H., and Miller R. H. (1992) Sequence analysis of the 5' noncoding region of hepatitis C virus. Proc Natl Acad Sci U S A. 89, 4942-4946

33 Kikuchi K., Umehara T., Fukuda K., Hwang J., Kuno A., Hasegawa T., and Nishikawa S. (2003) RNA aptamers targeted to domain II of hepatitis C virus IRES that bind to its apical loop region. J Biochem (Tokyo). 133, 263-270

34 Da Rocha Gomes S., Dausse E., and Toulme J. J. (2004) Determinants of apical loop-internal loop RNA-RNA interactions involving the HCV IRES. Biochem Biophys Res Commun. 322, 820-826

35 Kikuchi K., Umehara T., Fukuda K., Kuno A., Hasegawa T., and Nishikawa S. (2005) A hepatitis C virus (HCV) internal ribosome entry site (IRES) domain III-IV-targeted aptamer inhibits translation by binding to an apical loop of domain IIId. Nucleic Acids Res. 33, 683-692

36 Collier A. J., Tang S., and Elliott R. M. (1998) Translation efficiencies of the 5' untranslated region from representatives of the six major genotypes of hepatitis C virus using a novel bicistronic reporter assay system. J Gen Virol. 79 (Pt 10), 2359-2366

37 Piron M., Beguiristain N., Nadal A., Martínez-Salas E., and Gómez J. (2005) Characterizing the function and structural organization of the 5' tRNA-like motif within the hepatitis C virus quasispecies. Nucleic Acids Res. 33, 1487-1502

38 Kamoshita N., Tsukiyama-Kohara K., Kohara M., and Nomoto A. (1997) Genetic analysis of internal ribosomal entry site on hepatitis C virus RNA: implication for

involvement of the highly ordered structure and cell type-specific transacting factors. Virology. 233, 9-18

39 Honda M., Kaneko S., Matsushita E., Kobayashi K., Abell G. A., and Lemon S. M. (2000) Cell cycle regulation of hepatitis C virus internal ribosomal entry site-directed translation. Gastroenterology. 118, 152-162

40 Rijnbrand R. C., and Lemon S. M. (2000) Internal ribosome entry site-mediated translation in hepatitis C virus replication. Curr Top Microbiol Immunol. 242, 85-116

TABLE 1

IC_{50} values for the different inhibitory RNAs

Inhibitor	**IC_{50} (µM)[a]**	**Relative FLuc Synthesis[b]**
HH363-10	0.15 ± 0.04	11.22 ± 2.77
Ap10	1.95 ± 0.25	30.76 ± 11.60
HH363	3.46 ± 0.32	42.22 ± 6.32
HH363+Ap10	1.75 ± 0.41	32.39 ± 5.31

[a] IC_{50} values were derived from the equation $y = 100/(1 + 10^{(LogIC50-X)})$.

[b] Data correspond to the highest concentration of inhibitor tested. Values are the mean of at least three independent trials.

FIGURE LEGENDS

Figure 1. The HCV-IRES domain and HH363-10. A) Sequence and secondary structure of the HCV IRES. The cleavage site is indicated by an arrow. Nucleotides proposed to interact with HH363-10 are shown in bold and enlarged. Start codon is in italics. B) Sequence and secondary structure of HH363-10 predicted by experimental constraints and employing MFold software. Ribozyme HH363 is shadowed. Tertiary contacts predicted by PknotsRG are indicated by dotted lines. G nucleotides accessible to T1 under non-denaturing conditions are indicated by open (low), gray (medium) or filled triangles (high accessibility). Residues in the aptamer domain responsible for the interaction with domain IIIf of the IRES are shown in bold and enlarged. Encircled nucleotides were mutated as indicated to generate the respective inactive variants (HH363m-10, G_{14} → A; HH363-10m, $C_{49}GUA_{52}$ → GCAC; HH363m-10m, G_{14} → A and $C_{49}GUA_{52}$ → GCAC).

Figure 2. *In vitro* inhibition of IRES-dependent translation by the selected variants. The bar chart shows the reduction in FLuc synthesis achieved for each inhibitor RNA at a concentration of 5 μM, normalized with respect to the cap-dependent translation of RLuc mRNA. Values are referred to those obtained in the absence of inhibitor, and are the mean of at least three independent assays.

Figure 3. Specific *in vitro* inhibition of IRES function by HH363-10. The plot shows the reduction in FLuc synthesis normalized with the levels of RLuc protein. The IRES activity obtained at each concentration of inhibitor is represented as the percentage of the control

reaction in the absence of HH363-10. Data were fitted to a non-linear regression curve to determine the IC_{50} value and are the mean of four independent experiments.

Figure 4. Cleavage of IRES RNA in RRL. The graph shows the fraction of the internally radiolabeled 5'HCV-691 RNA substrate processed by different concentrations of either HH363-10 (open circles) or HH363 (filled circles) in the presence of rabbit reticulocyte lysate.

Figure 5. Probing assays of the IRES/HH363-10 complex. A) and B) show autoradiographs of the RNase H probing assays for 5'HCV-356 with the oligonucleotide asIRES305 (A) or asIRES196 (B). An amount of 50 fmol of the ^{32}P 5' end-labeled substrate was incubated with (+) or without HH363-10 in the presence of the probe oligonucleotide. Digestion reactions were initiated by the addition of 15 U of RNase H and extended up to 10 min. Specific cleavage products were resolved on a 6% high resolution denaturing polyacrilamide gel and are indicated by an arrow. T1L, T1 cleavage ladder. C) The fraction of RNase H cleavage product at different concentrations of HH363-10 is represented.

Figure 6. Secondary structure analysis of HH363-10 and identification of the interacting residues with the IRES. A) ^{32}P 5' end-labeled HH363-10 was partially digested with RNase T1, RNase A or Pb^{2+}, either in the absence (-) or presence (+) of the substrate RNA 5'HCV-691gg. The right panel shows a more detailed view of the cleavage pattern for the aptamer domain. Residues participating in the pseudoknot structure are indicated by an

asterisk. The arrows show nucleotides $G_{41}AG_{43}$. T1L, T1 cleavage ladder. OH, alkaline ladder.

Figure 7. HH363-10 and Ap10 prevent the assembly of the 80S ribosomal particle. Sucrose gradient sedimentation profiles of ^{32}P-internally labeled IRES-FLuc mRNA incubated in RRL in the absence and presence of a 125-fold molar excess of inhibitor RNAs (HH363-10, Ap 10 or HH363) or 2 mM of GMP-PNP. Filled circles, control reaction profile; open circles, sedimentation profile with the inhibitor. In all cases, the percentage disintegrations are represented against the corresponding gradient fraction number. The 48S and 80S complexes are indicated. Fractions were collected from the top downwards.

Figure 8. Inhibition of IRES-dependent translation by HH363-10 in Huh-7 cells. Huh-7 cells were co-transfected with different amounts of inhibitor RNAs and 1.5 μg of a mix containing the transcripts IRES-FLuc and RLuc. The collection of mutants was obtained by the introduction of variations in HH363-10 nucleotidic sequence as indicated in figure 1. IRES function is measured as the activity of FLuc protein and referred to that obtained for RLuc. Luciferase activity in the control reactions is established as 100%. Data points are the mean of three independent experiments.

Figure 1A

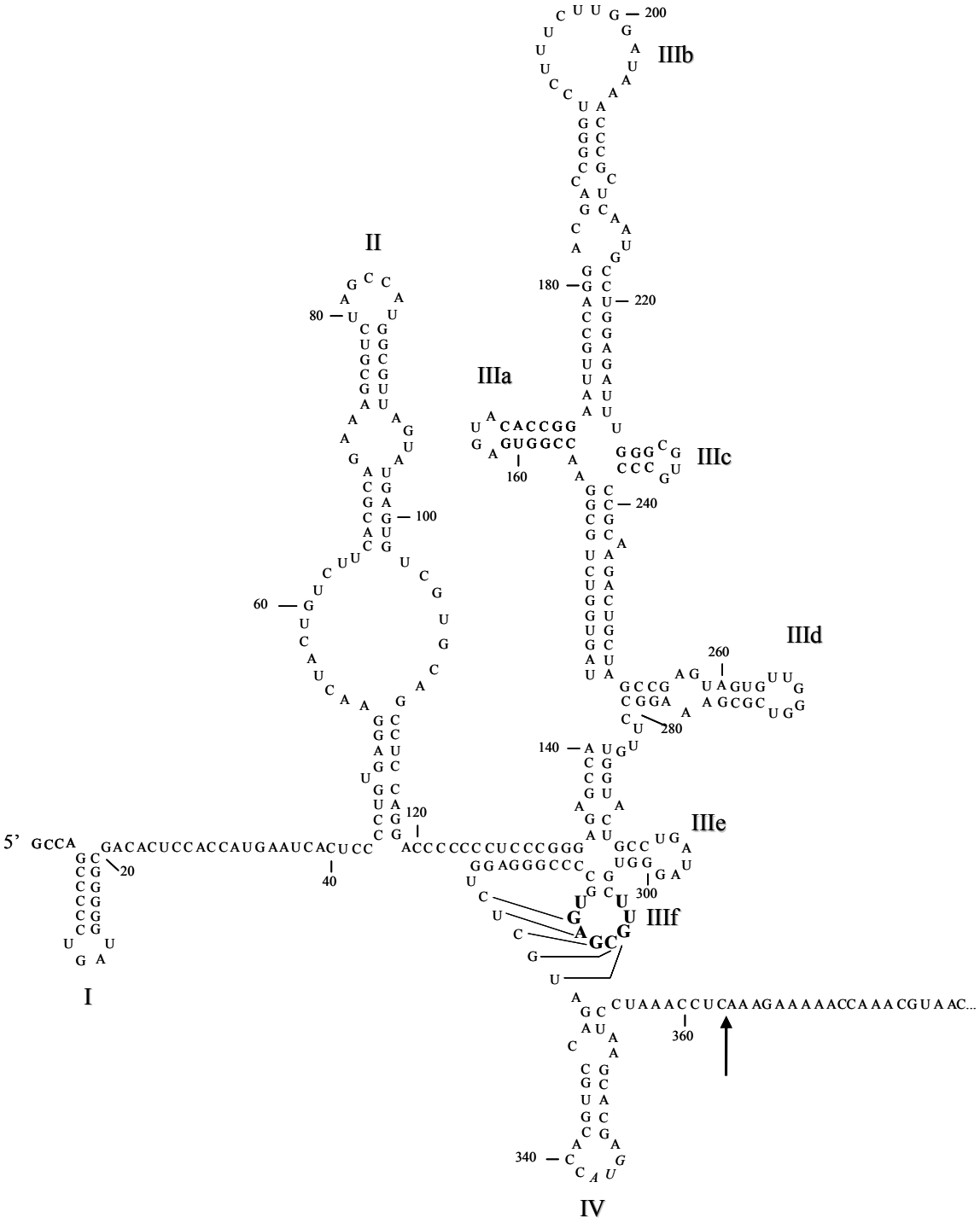
I
II
IIIa
IIIb
IIIc
IIId
IIIe
IIIf
IV
5' GCCA
GACACUCCACCAUGAAUCACUCC
ACCCCCCCCUCCCGGG
GCCUGA
UGGGAU
CUAAACCUCAAGAAAAACCAAACGUAAC...
CACCGG
GUGGCC
GGGCG
CCCG
AGUGUUG
AGCGCUGG
GCCG
CGGA
AUGG
UGGA
20
40
60
80
100
120
140
160
180
200
220
240
260
280
300
340
360

Figure 1B

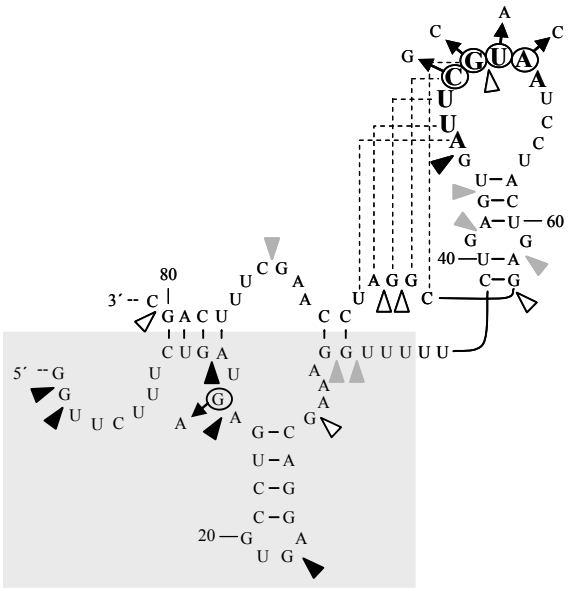

Figure 2

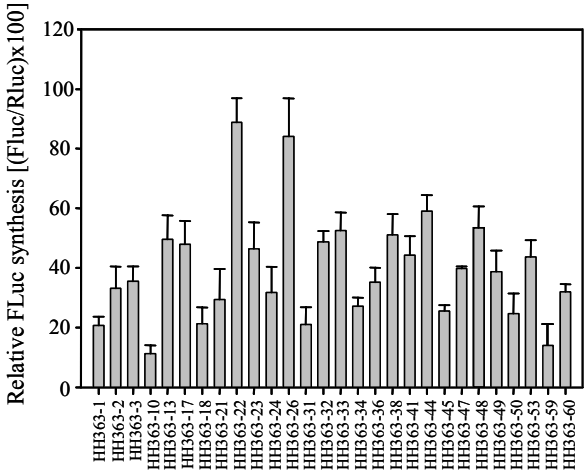
Relative FLuc synthesis [(Fluc/Rluc)x100]
120
100
80
60
40
20
0
HH363-1
HH363-2
HH363-3
HH363-10
HH363-13
HH363-17
HH363-18
HH363-21
HH363-22
HH363-23
HH363-24
HH363-26
HH363-31
HH363-32
HH363-33
HH363-34
HH363-36
HH363-38
HH363-41
HH363-44
HH363-45
HH363-47
HH363-48
HH363-49
HH363-50
HH363-53
HH363-59
HH363-60

Figure 3

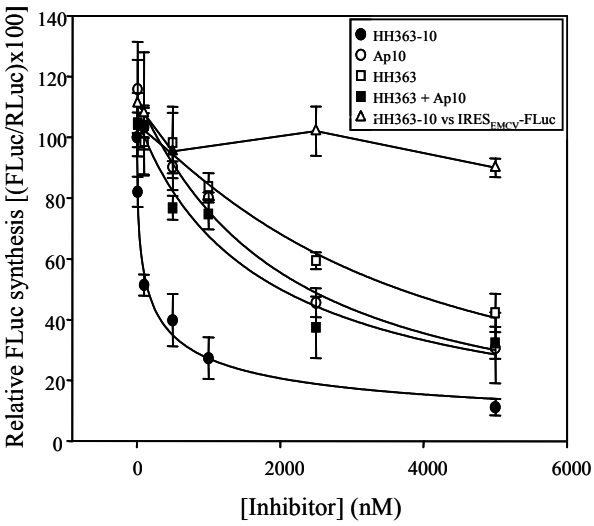
Relative FLuc synthesis [(FLuc/RLuc)x100]
140
120
100
80
60
40
20
0
0
2000
4000
6000
[Inhibitor] (nM)
HH363-10
Ap10
HH363
HH363 + Ap10
HH363-10 vs IRES$_{EMCV}$-FLuc

Figure 4

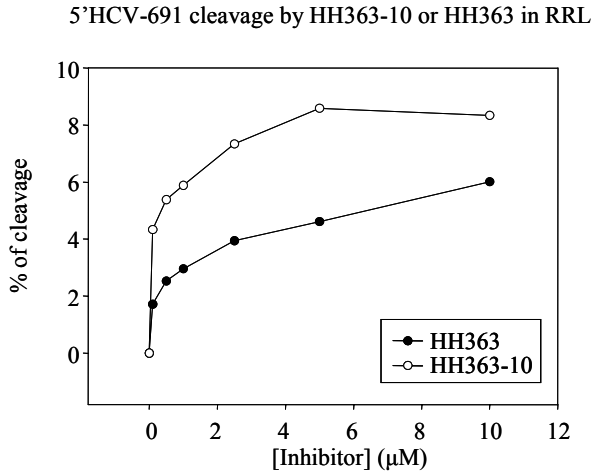
5'HCV-691 cleavage by HH363-10 or HH363 in RRL
% of cleavage
[Inhibitor] (μM)
HH363
HH363-10
0
2
4
6
8
10
12

Figure 5

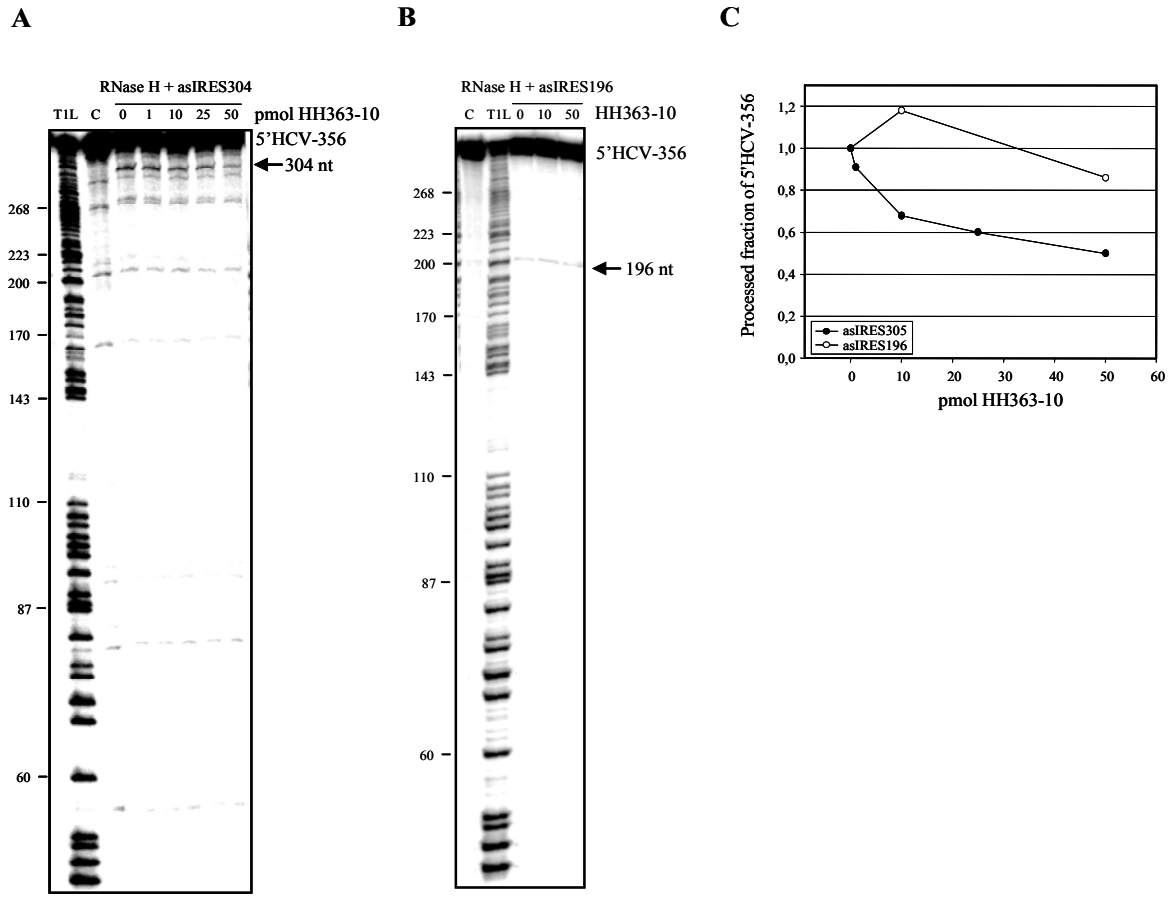
A
B
C
RNase H + asIRES304
T1L C 0 1 10 25 50 pmol HH363-10
5'HCV-356
304 nt
268
223
200
170
143
110
87
60
RNase H + asIRES196
C T1L 0 10 50 HH363-10
5'HCV-356
196 nt
268
223
200
170
143
110
87
60
Processed fraction of 5'HCV-356
1,2
1,0
0,8
0,6
0,4
0,2
0,0
asIRES305
asIRES196
0 10 20 30 40 50 60
pmol HH363-10

Figure 6

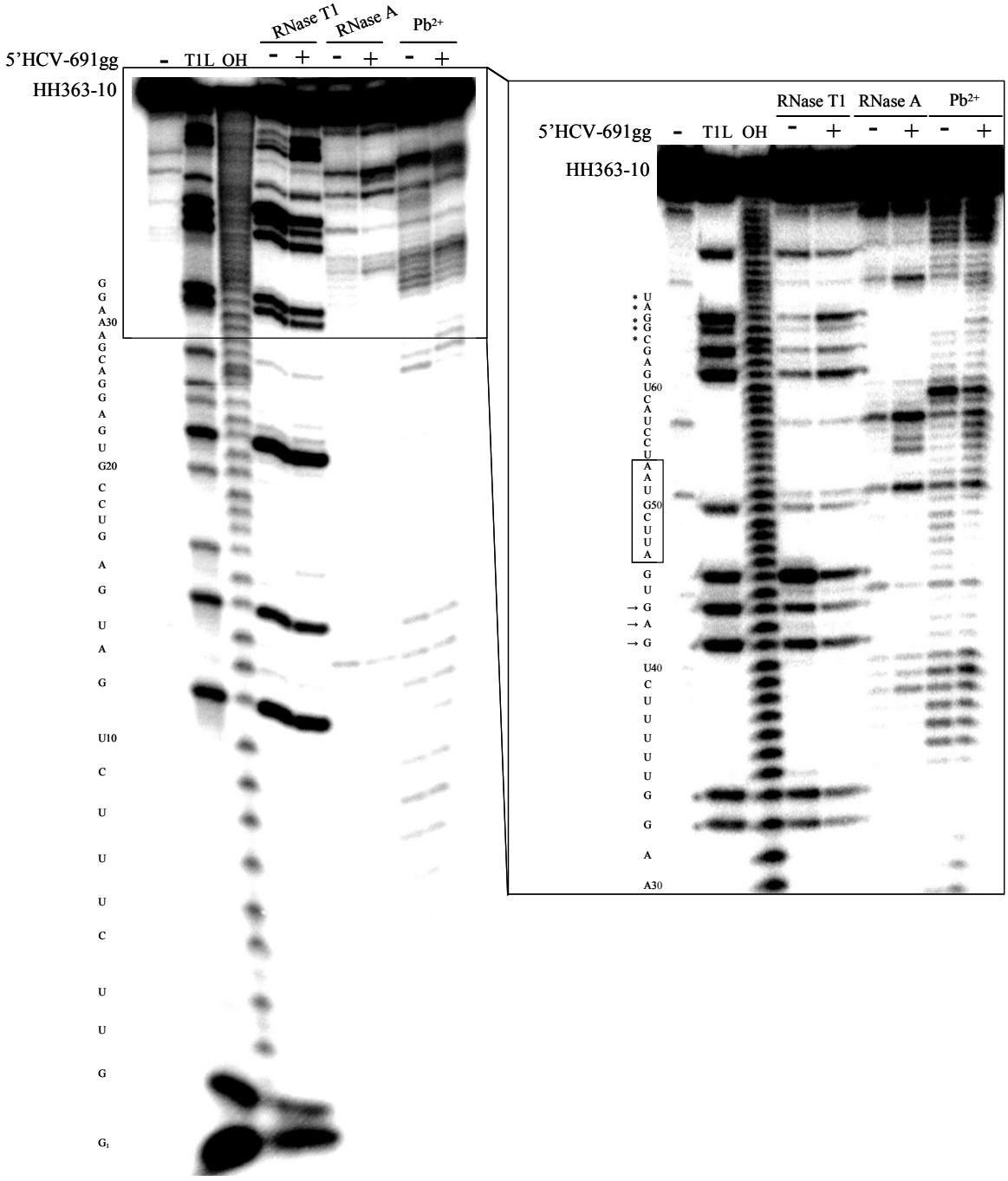
RNase T1
RNase A
Pb2+
5'HCV-691gg
- T1L OH - + - + - +
HH363-10
G
G
A
A30
A
G
C
A
G
G
A
G
U
G20
C
C
U
G
A
G
U
A
G
U10
C
U
U
U
C
U
U
G
G1
RNase T1
RNase A
Pb2+
5'HCV-691gg
- T1L OH - + - + - +
HH363-10
* U
* A
* G
* G
* C
G
A
G
U60
C
A
U
C
C
U
A
A
U
G50
C
U
U
A
G
U
→ G
→ A
→ G
U40
C
U
U
U
U
G
G
A
A30

Figure 7

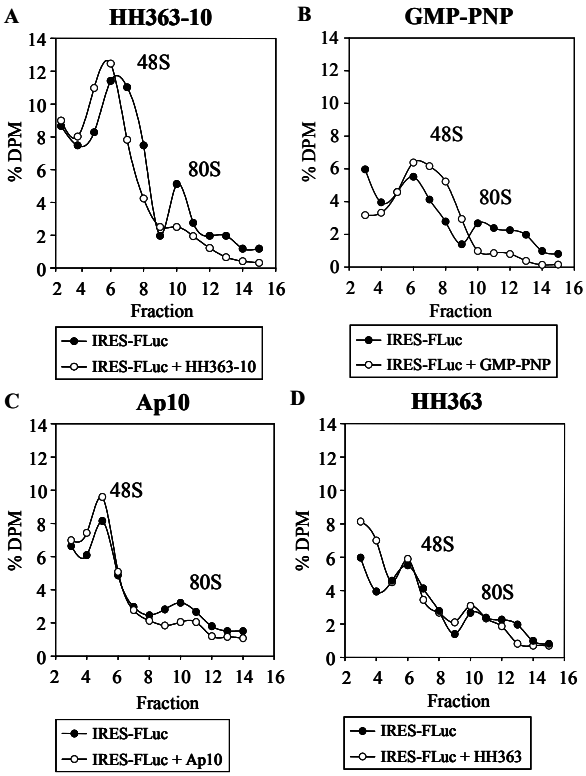
A
HH363-10
48S
80S
% DPM
Fraction
IRES-FLuc
IRES-FLuc + HH363-10
B
GMP-PNP
48S
80S
% DPM
Fraction
IRES-FLuc
IRES-FLuc + GMP-PNP
C
Ap10
48S
80S
% DPM
Fraction
IRES-FLuc
IRES-FLuc + Ap10
D
HH363
48S
80S
% DPM
Fraction
IRES-FLuc
IRES-FLuc + HH363

Figure 8

.

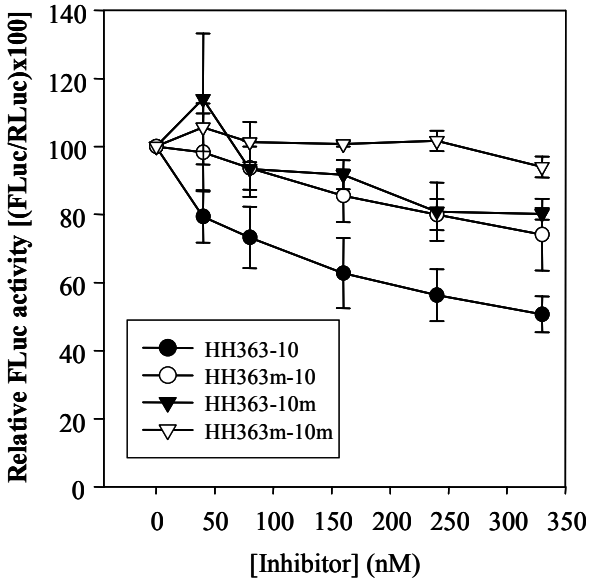
Relative FLuc activity [(FLuc/RLuc)x100]
140
120
100
80
60
40
20
0
0
50
100
150
200
250
300
350
[Inhibitor] (nM)
HH363-10
HH363m-10
HH363-10m
HH363m-10m